SMALL DIAMETER FIBRES AS NEW WICK MATERIAL FOR CAPILLARY-DRIVEN HEAT PIPES

De Schampheleire S.*, De Kerpel K., Deruyter T. and De Paepe M.
*Author for correspondence
Department of Flow, Heat and Combustion Mechanics,
Ghent University,
9000 Ghent
Belgium,
E-mail: Sven.DeSchampheleire@ugent.be

ABSTRACT

Heat pipes with a wick material consisting of small diameter metal fibres of 12 µm are investigated. The container material is copper and the working fluid is water. The fibre mesh heat pipe is compared with two other wick structures: a screen mesh (145 meshes per inch) and a sintered powder wick. All three heat pipes have an outer diameter of 6 mm, a length of 200 mm. The heat pipes are tested in a vertical orientation, both gravity-opposed and gravity-assisted. In the gravity-opposed orientation the heat pipes are tested for a heat input up to 50 W and an operating temperature of 70°C. In the gravity-assisted orientation the heat pipes are tested up to 160 W and 120°C. The thermal resistance and the temperature difference between evaporator and condenser are used as performance indicators.

For the gravity-assisted orientation, the screen mesh wick clearly outperforms the fibre and sintered powder wick, due to its higher permeability and better ability to distribute the working fluid over the circumference of the wick. For the gravity-opposed orientation, the fibre and screen mesh heat pipe perform equally well. Both have a lower thermal resistance than the sintered powder heat pipe, as the small diameter fibres and fine mesh create more and very small capillary channels in comparison with the sintered powder wick.

INTRODUCTION

A heat pipe has the advantage over other conventional methods that it can transport heat over a considerable distance with no additional power input to the system. Figure 1 illustrates the working principle of a capillary-driven heat pipe with a circular cross section. When one end of the heat pipe is heated, the local liquid will start to evaporate. Vapour is transported towards the other side of the heat pipe, where it condenses against a cooled surface. If the heat pipe is placed vertically with the condenser at the top and the evaporator at the lower end, the liquid formed in the condenser will naturally flow back to the evaporator due to gravity. In this work, this orientation will be called the gravity-assisted orientation of the heat pipe. If the condenser is located at the lower end and the evaporator at the top - this is called the gravity-opposing case- the wick material induces the capillary forces which transport the liquid (again) to the evaporator. The section between the evaporator and the condenser is called the adiabatic section. In theory, a heat pipe is an isothermal device because evaporation and condensation occur at the same temperature. In practice, a lot of thermal resistances are present over the heat pipe and a temperature difference between the two ends of a heat pipe exists. In the reference textbook of Reay et al. [1] those thermal resistances are described. One of these resistances is the resistance due to the wick material ($\boldsymbol{R_w}$). It can be calculated through Eq. 1. However, the effective conductivity of the wick ($\boldsymbol{k_{eff}}$) is mostly unknown. Therefore, a total thermal resistance ($\boldsymbol{R_{tot}}$) of the heat pipe is reported frequently.

$$\frac{\ln\left(\frac{D_1}{D_2}\right)}{2\pi k_{eff} L} \tag{1}$$

In this paper we will focus on the effect on the wick material on the total thermal resistance of the heat pipe.

NOMENCLATURE

D_1	$[m]$	inner diameter
D_2	$[m]$	outer diameter
k	$[W/mK]$	thermal conductivity
K	$[m^2]$	permeability
L	$[m]$	length of the evaporator and condenser (in this work both have the same length)
$\dot{Q}$	$[W]$	heat transfer rate
R	$[K/W]$	thermal resistance
T	$[K]$	temperature

Greek symbols

ϕ	$[-]$	porosity

Subscript

con	condenser
e	evaporator
eff	effective
evap	evaporator
max	maximum
paste	thermal paste
tot	total, overall, equivalent

WICK MATERIALS

The number of possible wick types is virtually endless. In this study, the focus is on homogeneous wick designs capable of performing against gravity. A sintered powder, a wrapped screen mesh and randomly stacked small diameter fibres are studied as wick structures, in this section, these structures are discussed in more detail.

Sintered powder wicks are regarded as a promising candidate for high heat flux applications because of their high capillary pressure, which can be attained by its small pore radius. The sintered metal wicks are manufactured by packing small metal particles between the container and a mandrel. The mandrel is discarded after the sintering process. A screen mesh wick consists out of several layers of screens woven out of metal thread. Usually three screens are rolled together and placed in the container of the heat pipe. The screens are then sintered to the container. There is a small increase in thermal resistance when increasing the number of screens, however, the maximum heat transfer also increases [2]. The larger the number of meshes per square inch, the lower the pore radius and permeability and the higher the capillary pressure. Wang et al. [3] stated that the maximum heat transfer capacity is affected by the mesh number, the wire diameter, number of layers, orientation of the heat pipe and sintering process. The influence of the orientation of the heat pipe on the maximum heat transfer capacity decreases with the number of layers used [3]. In general, screen wicks transfer more power (as they have a higher permeability), but sintered powder wicks have lower thermal resistance, higher heat flux capability and work better against gravity for heat pipes length past 150 mm [1].

Fibres as wick materials for heat pipes are also not new. In both review papers of Vasiliev [4] and Faghri [5] fibres are included into their list of used wick structures. At Fujikura® [6] so-called "super fibre heat pipes" were tested, with fibre diameters of the between 0.05 and 0.1 mm. The authors looked specifically to notebook applications in a vertical orientation. They stated that this new wick structure should provide smaller capillary channels with small effects on the heat pipe permeability. The authors used 4 mm OD heat pipes and tested up to evaporator input powers of 16 W. Thermal resistances as low as 0.5°C/W in vertical orientation are observed, which is 2 to 5 times better than conventional heat pipes, as stated by the authors.

The objective of this study is to experimentally investigate fibres a wick structure with even smaller diameters (12 µm). The performance of this fibre heat pipe will be compared to a sintered screen mesh heat pipe and a sintered powder heat pipe. All three heat pipes have a fixed outer diameter and length, 6 mm and 200 mm respectively. To manufacture the fibres, there is a cooperation with the Belgian company NV Bekaert SA.

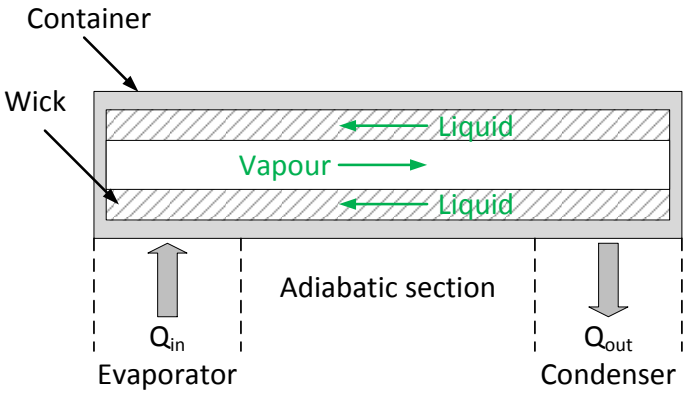

Figure 1 Illustration of the working principle of a heat pipe

TEST RIG

Tested Heat Pipes

The heat pipes with screen mesh wick and fibre wick were custom made by an external company specialised in heat pipes. A commercially available off-the-shelf heat pipe with a sintered powder wick with the same container dimensions and working fluid is also tested as a reference.

The screen mesh consists of 3 layers of a 145 meshes per inch screen. The wire diameter is 55.88 µm, with an opening size of 101.6 µm. The wick consists of three mesh layers with a total thickness of 0.4 mm. The three mesh screens are stacked together, rolled up, placed into the container of the heat pipe and sintered to the container. The porosity (ϕ) of the mesh screen is 46%.

For the fibre wick, the Cu12-fibres have a diameter of 12 µm. They are first randomly stacked upon each other and sintered to a screen with a thickness of 0.1 mm. Then four of those screens are stacked on to each other to obtain the same thickness as the screen mesh wick (0.4 mm). The fibre wick is placed in the heat pipe without further sintering. Hence, there is no metallic bond between fibre wick and copper tube as opposed to the screen mesh heat pipe. The porosity (ϕ) of the fibre screen is 37.9%. Both the fibre wick heat pipe and the mesh screen wick heat pipe are filled with 1.045 g of water.

The manufacturer of the commercially available sintered powder wick heat pipe is not willing to disclose the precise porosity of the wick material. However, the information in the literature on sintered powder wick heat pipes indicate that the porosity will be in the range of 29-35% [1], which is in any case lower than the other two tested wick materials.

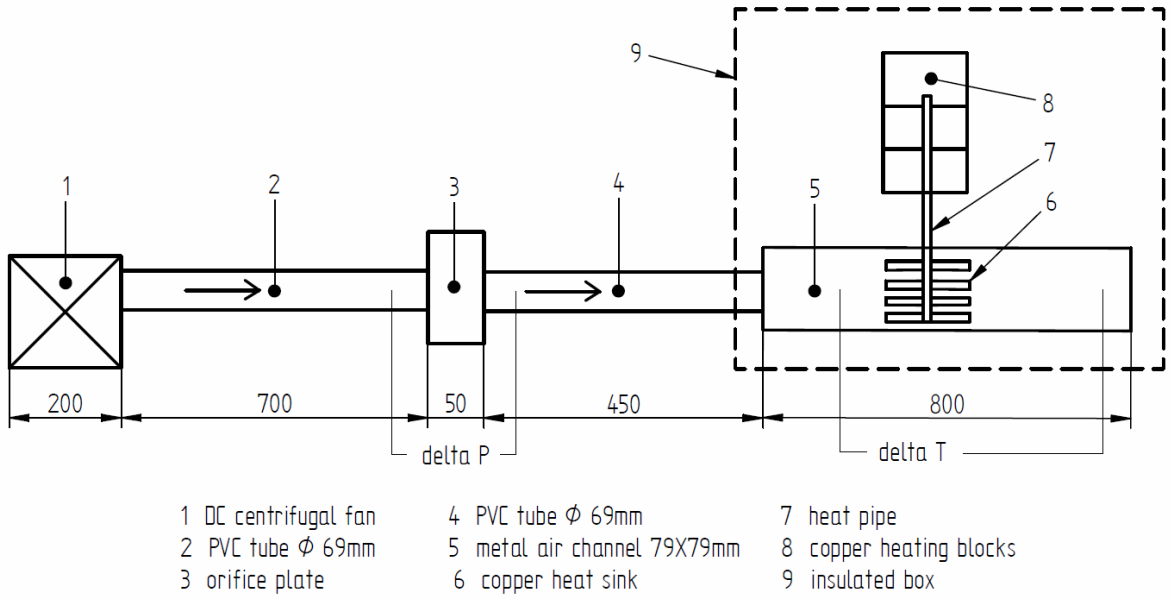

Figure 2 Schematic representation of the test assembly

Overview of the Test Facility

Figure 2 depicts a schematic representation of the test assembly. The setup consists of 2 main parts. One part consists of an insulated box which contains the heat pipe (Fig. 2, (7)), three copper blocks (one consisting of a band heater) (Fig. 2, (8)) and a copper heat sink on the condenser side of the heat pipe (Fig. 2, (6)). A detailed view of this insulated box is given in Fig. 2. The second part of the setup contains the air supply to the heat sink at condenser side of the heat pipe. It consists of a centrifugal fan (Fig. 2, (1)) and an orifice plate (Fig. 2, (3)) over which the airside mass flow rate is measured according to the ISO 5167:1-1991 Standard [7]. As cited in this standard, the upstream straight length and downstream straight length have to be 10D and 5D respectively. The heat pipes are tested in two orientations: gravity-assisted and gravity-opposed orientation. This is possible because the frame with the insulated box can be turned over 180°. In this work, forced convective air cooling is used in order to attain a better closure of the heat balance, in comparison with water. This is due to the lower heat capacity of air compared to water, resulting in a higher temperature difference which allows more accurate measurement.

Evaporator Side

A detailed view of the evaporator side of the heat pipe is shown in Figure 3. There are three cylindrical copper blocks (OD: 51 mm) stacked upon each other. Each block has a different height: 10, 20 and 40 mm. Around the copper block of 40 mm a mineral insulated band heater with a height of 30 mm and a maximum heating power of 350 W is used. In the copper blocks, small grooves with a width and depth of 0.5 mm are machined. In these grooves, K-type thermocouples with a diameter of 0.5 mm are mounted in order to measure the temperature of the thermal blocks. The thermocouples are fixed in such a way that they touch the wall of the heat pipe, as shown in Figure 3. In total four thermocouples are used to measure the temperature at the evaporator (T_e). In the center of the copper cylinders a hole with a diameter of 6.1 mm is made in which the heat pipe is placed. When mounting the heat pipe, thermal paste is applied to fill any possible gaps. Furthermore, two other holes are machined in the cylinders. In these holes, two metal threaded rods with a diameter of 6 mm are placed to hold the evaporator in place when the frame with the insulated box is turned over 180°.

To minimize the heat losses, four guard heaters are used. The guard heaters consist of etched foil silicone rubber heaters with a heater power of 15 W. The dimensions of the heaters are 100x150 mm², with a thickness of 1.5mm. Stick-on K-type thermocouple with a dimension of 20x12 mm² are used to measure the temperature on the guard heaters. To minimize the heat losses of the main heater, the temperature of the guard heaters is set to the same temperature as the main heater. This guarantees that all the heat applied to the main heater will be transferred to the heat pipe. Additionally, a large amount of insulation material is added around the heaters. Three types of insulation material are used. The Microtherm® insulation plates are custom made to size. These plates can withstand temperatures up to 1000°C and have a very low thermal conductivity (0.021 W/mK). The Eurofloor® insulation material is considerably less expensive and has a similar thermal conductivity, but can only withstand temperature up to 100°C. The flexible Promaglaf® blankets (with a slightly higher thermal conductivity: 0.06 W/mK) are used to close the airgaps between the Eurofloor® and Microtherm® plates.

The support of the evaporator is mounted on the wooden plate. This support is made out of Pertinax. Pertinax is a synthetic resin bonded paper which has a low thermal conductivity (0.2 W/mK) and can withstand temperatures up to

120°C. Above the support, a layer of Microtherm® insulation with a thickness of 10 mm is placed. This layer of insulation material separates the evaporator from the adiabatic section. At the top of the copper blocks, an additional steel plate is mounted. This plate is necessary to hold the heat pipe in position. This is done with a small bolt at the top which can be adjusted to fix the heat pipe.

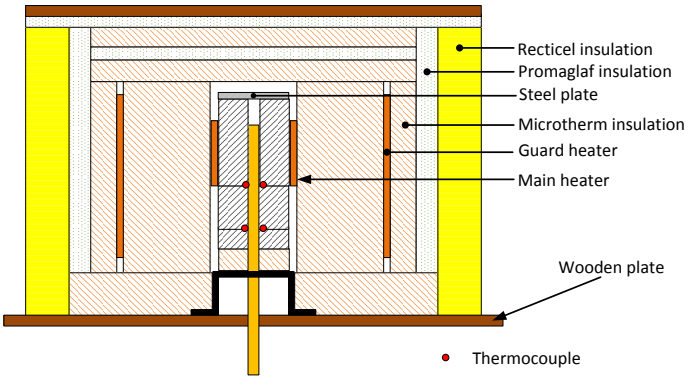

Figure 3 Detailed view of the evaporator side of the heat pipe

Condenser Side

The condenser side of the heat pipe is mounted in a heat sink. The heat sink is necessary to dissipate the energy added by the band heater to the environment. The heat sink (Fig. 2, (6)) is made out of a solid block of copper. In total 10 rectangular fins are machined with a fin thickness of 2 mm. In the middle of the heat sink, a hole with a diameter of 6.1 mm is made in which the heat pipe can fix. Again thermal paste is used to minimize the thermal resistance. At the top of the heat sink, two small holes are made with a diameter of 1 mm. In these holes, two K-type thermocouples with a junction diameter of 1 mm are fixed to measure the temperature of the heat sink. The average of this temperature represents the temperature of the condenser (T_C). The heat sink is mounted in the air channel such that the flow downstream of the heat sink is uniform. It is verified by 2D hot wire measurements at the end of the test section that the velocity differences over the test section are smaller than 5%.

On the airside of the heat sink, one K-type thermocouple is used to measure the uniform temperature before the heat sink, while six K-type thermocouples (with a junction diameter of 0.5 mm) are used to measure the temperature after the heat sink. In this way, the heat balance between $\dot{Q}_{in}$ and $\dot{Q}_{out}$ can be measured and was for all measurements smaller than 3%. This ensures the heat losses to the environment are limited.

The condenser and evaporator length is chosen to be the same (60 mm).

TEST PROCEDURE

In this work the heat sink is cooled down with a constant air mass flow rate. The total thermal resistance is frequently taken as a performance parameter and is calculated through Eq. 2. Steady-state is attained if the standard deviation of the last 120 temperature readings is lower than 0.08°C. Due to the large amount of insulating material in the setup, it takes between 1 and 1.5 hours before steady-state is reached for one set point. A dataset is obtained by sampling all relevant quantities during 150 s at a sampling rate of 1 Hz, in this way the average temperature is determined by averaging over 150 measurements.

$$R_{tot} = \frac{T_e - T_c}{\dot{Q}_{in}} \quad (2)$$

In order to assess the quality of the measurements, a thorough uncertainty analysis was performed. Standard error propagation rules as described by Moffat [8] were used to calculate the overall uncertainty (root-sum-square method). The tolerance on the machined parts of the test rig is ± 0.05 mm. Note that all uncertainties in this work are expressed as 95% confidence intervals.

Prior to the measurements, all thermocouples were calibrated using a Druck DBC150 temperature calibrator furnace to eliminate systematic errors. The reference temperature is measured with a FLUKE 1523 PT100 with an accuracy of 0.068°C. The resulting uncertainty on all used temperatures varies between 0.15 °C and 0.25 °C, conservatively. The pressure drop over the orifice plate is measured with a pressure transducer of Halstrup Walcher® with a pressure range between 0 and 250 Pa. The pressure transducer is calibrated to an uncertainty of ±0.2% of the total measuring range.

The uncertainty of the input power is mainly dependent on the accuracy of the transducer. The voltage transducer has an accuracy of 0.5% which results in an absolute error of 0.1V, while the current transducer has an accuracy of 0.5%, resulting in an absolute error of 0.004 A. For low input powers the uncertainty is quite high (relative uncertainty ± 6%), but as soon as the input power is higher than 25 W, the relative uncertainty of the input power falls below 3%.

For the uncertainty on the temperatures and temperature differences also the uncertainty due to the layer of thermal paste is taken into account, between the heat pipe and the evaporator (copper cylinders) and between the heat pipe and the condenser (heat sink) respectively. Therefore, the uncertainty on the condenser and evaporator length is taken 1 mm and the uncertainty on the thermal conductivity of the paste is taken 0.2 W/mK (25% relative uncertainty). This leads to high uncertainty values for $(T_e - T_c)$, however it is a conservative estimation of the uncertainty.

RESULTS AND DISCUSSION

Results in Gravity-opposing Direction

In the gravity-opposing direction, the airside velocity is fixed at 0.5 m/s, corresponding with a mass flow rate of 0.0044 kg/s. The screen mesh and fibre heat pipe are gradually tested up to 50 W power input, in steps of 5 W. For the sintered powder heat pipe, some additional points where tested in the low power range in order to get a more detailed view.

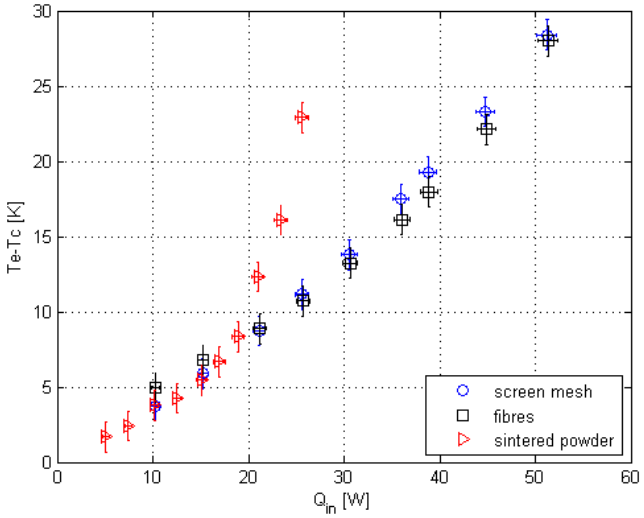

Figure 4 Temperature difference $T_e - T_c$ against the input power for the gravity-opposing direction

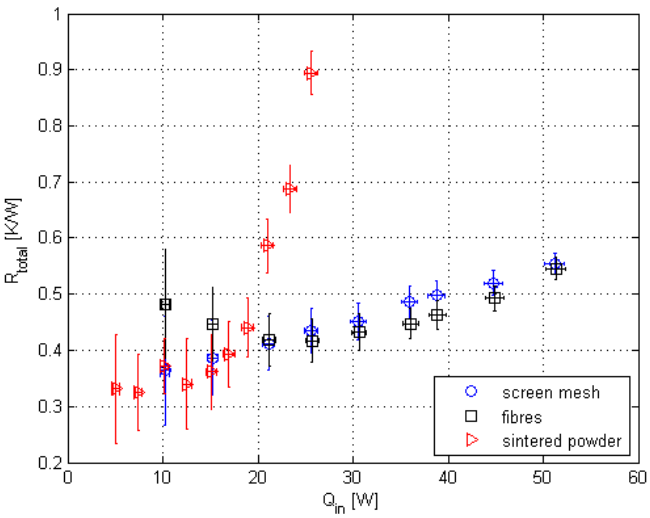

Figure 5 Total thermal resistance against the input power for the gravity-opposing direction

In Figure 4 the temperature difference between the evaporator and the condenser is plotted as function of the heat input. The general trend is clear. When the amount of power added by the band heater increases, the temperature difference $T_e - T_c$ also increases, as $T_e - T_c$ is the driving force for the heat transfer. It can be seen that for a heat transfer rate below 20 W, the difference between the heat pipes is insignificant. For power ranges above 20 W, the sintered powder heat pipe performs the worst of all the tested heat pipes. The screen mesh and the fibre heat pipe show a similar performance. The point of dry-out can clearly be recognized for the sintered powder heat pipe. This is the point where $T_e - T_c$ shows an increase in slope. As mentioned earlier, the dry-out point is the point where the capillary pumping power of the wick structure cannot deliver enough working fluid to the evaporator. The consequence is that the evaporator temperature increases because the heating power is superheating the vapour instead of generating saturated vapour from liquid. This point of dry-out is still not reached for a heat transfer rate of 50 W in case of the fibre and the screen mesh heat pipe.

In Figure 6 the thermal resistance is plotted as a function of the heat transfer rate for the three tested heat pipes. The same conclusion as for Figure 5 holds. For high heat transfer rates, there is no significant difference between the screen mesh and the fibre heat pipe. No conclusions can be drawn when the thermal resistance is taken as a performance indicator for low heat transfer rates. Assuming a threshold thermal resistance of 0.55 K/W, the sintered powder heat pipe transfers 20 W of energy, while the other two heat pipes can transfer 50 W.

These results are comparable to the open literature where values of the thermal resistance between 0.3 and 0.6 K/W are commonly found in Wong and Chen [9] and Weibel et al. [10]. The shape of the thermal resistance as a function of the heat input can be explained as follows Reay et al. [1]. The total thermal resistance is basically the equivalent resistance of several smaller resistances: contact resistance, resistance through thermal conduction over container material in radial direction, resistance due to the temperature drop over the liquid-vapour interface, resistance over the wick structure, resistance over the thermal paste… For the sake of simplicity, an equivalent evaporator and condenser thermal resistance can be defined by R_{evap} and R_{con} respectively, then the total thermal resistance of the heat pipe is the sum of both equivalent resistances. Since the thermal conductivity of the thermal paste is constant, the influence of the thermal resistance of the layers of thermal paste R_{paste} is also constant. Furthermore, as the condenser and evaporator have the same length, the total resistance of both thermal paste layers (as can be calculated similar to Eq. (1)) is equal and amounts 0.08 K/W. This indeed makes up a significant part of the total thermal resistance, which varies between 0.32 and 0.9 K/W. However, the use of thermal paste is inevitable when studying heat pipes in such a test rig.

Li et al. [11] analytically and experimentally proved that the R_{con} is approximately constant because the heat transfer in the condenser is by conduction. So the behaviour of the equivalent thermal resistance (R_{tot}) can be explained based on the behaviour of R_{evap}. This behaviour is extensively explained by Weibel et al. [10]. R_{evap} will increase steadily for a high heat input, due to the existence of dry-out conditions in some specific regions in the evaporator, creating some localized vapour blankets in the evaporator. As these vapour blankets have a lower thermal conductivity, the thermal resistance of the heat pipe will increase. However, due to their localized nature, the heat pipe will still perform acceptably, until these vapour blankets cover the complete surface of the evaporator (dry-out condition).

The occurrence of localized dry patches in the evaporator explains why the thermal resistance of the sintered

powder heat pipe stays constant for low power inputs, and then slightly increases. This is the early start of dry-out. At a heat input of 20 W, there is a sudden and strong increase in thermal resistance observed. This is the real dry-out point. For the screen mesh wick heat pipe, the thermal resistance steadily increases from 10 to 50 W heat input.

For the fibre heat pipe, a similar behaviour is seen for a heat input above 20W, however, the thermal resistance decreases with an increase in heat input for low heat inputs. This initial decrease with input power is non-significant with the present setup; further measurements are needed to verify whether it really occurs. The behaviour (based on the average measurement points) is explained by the work of Weibel et al. [10]. They conducted experiments on the vapour formation regimes of a sintered powder heat pipe and stated that there are two main regimes of heat transport which they called the evaporation regime and the boiling regime. The authors observe that at low heat transfer rates the evaporation regime is dominant to the boiling regime. When the heat transfer rate increases, however, the boiling regime gets more important. The evaporation regime is present as long as the wick is fully saturated with liquid.

The evaporation regime consists of three resistances in series: the resistances through the container wall, the wick conduction resistance and the thin-film evaporation resistance at the free surface meniscus. It is stated in Weibel et al. [10] that the wick thermal resistance and the resistance through the wall are the most significant ones. Thus, in the evaporation regime, the total resistance is large because of the large wick conduction resistance. In the boiling regime, heat transfer occurs by the formation of bubbles. The nucleation of these bubbles occurs at the hottest part of the wick layer: at the heat pipe wall. In this way, the large wick conduction resistance is eliminated. The consequence is that the overall thermal resistance in the boiling regime is significantly reduced in comparison to the resistance in the evaporation regime. For heat inputs higher than 20 W, the thermal resistance is again increased because of the occurrence of dry patches.

The fibre heat pipe is far better in performance than the sintered powder heat pipe in the gravity opposed orientation. In comparison with a screen mesh heat pipe, however, the fibre heat pipe performs similar in the gravity-opposed direction. This is because of the small capillary channels that are created by the small diameter fibres (high capillary pressure).

Results in Gravity-assisting Direction

For the gravity-assisted direction, the velocity of the air flow is constant at 1 m/s at the test section. This results in a mass flow rate of 0.0084 kg/s. The mass flow rate is higher than for the gravity-opposing direction; this is because dry-out appears at a much higher heat transfer rate and the cooling rate at the condenser has to be high enough. The heat inputs are gradually increased to 160 W. When reaching 160 W, the evaporator temperature closely reached 150°C which is the maximum service temperature of the used thermal paste. In the gravity-assisted direction, higher heat inputs can be tested, as the heat pipe is able to transfer more heat.

In Figure 6 the temperature difference between the evaporator and the condenser is plotted as function of the heat input at the evaporator. Again this temperature difference increases with increasing heat input. For heat inputs smaller than 60-80 W, the sintered powder heat pipe performs significantly better than the screen mesh and fibre heat pipe. However, above a heat input of 60 W, the screen mesh heat pipe shows the best performance and the sintered powder one performs worst. This specific behaviour can be expected based on the wick structure that is used. Especially in the gravity-assisted orientation, the permeability of the wick is very important to facilitate an easy return of the liquid to the evaporator. In this orientation, the capillary pressure is less important. As the porosity is higher for the screen mesh wick (46%) in comparison with the sintered powder (<35%) and fibre mesh (37.9%), the permeability is higher for this screen mesh. Furthermore, the higher permeability is provided by the

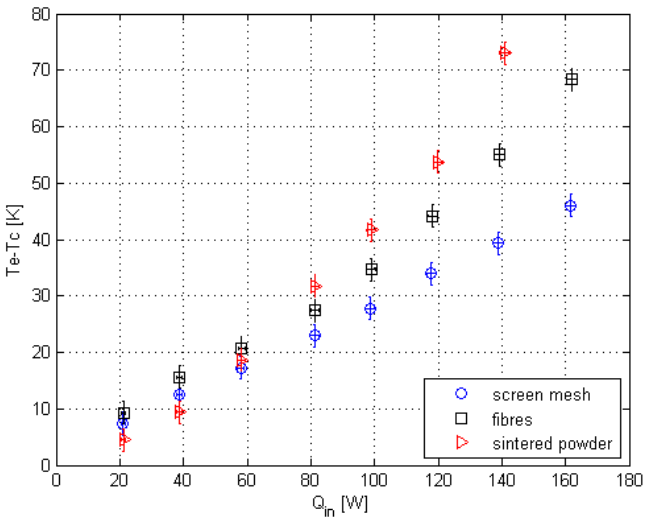

Figure 6 Temperature difference $T_e - T_c$ against the input power for the gravity-assisting direction

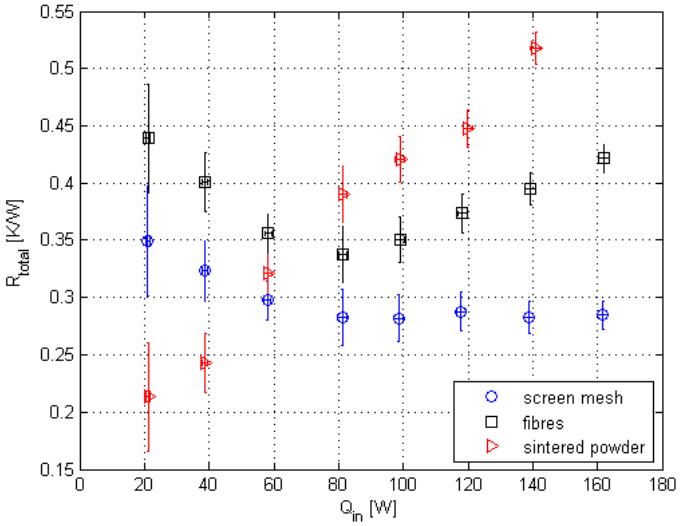

Figure 7 Total thermal resistance against the input power for the gravity-assisting direction

use of three separate screen layers because the fluid can flow between these separate layers. This is especially important as the high mesh size (145 meshes/inch) results in small pore sizes, resulting in a high capillary pressure.

In Figure 7, the thermal resistance is plotted as function of the heat input. The screen mesh heat pipe shows a trend similar to the experimental results presented by Li et al. [11] and Weibel and Garimella [12]. Both the fibre and the screen mesh heat pipe show a decreasing thermal resistance for low heat inputs. This is caused by the increasing importance of the boiling regime of two-phase heat transfer relative to the evaporation regime (as explained for the gravity-opposing orientation). However some remarkable trends are observed.

For heat inputs larger than 80 W, the trends for the screen mesh heat pipe and the fibre heat pipe are different. The thermal resistance of the screen mesh remains constant at 0.28 K/W while the fibre heat pipe starts to increase. The reason for this is given in Reay et al. [1]. The wick should be able to distribute the working fluid adequately over the circumference of the wick. The screen mesh wick with higher permeability will nicely distribute the working fluid over the wick and the thermal resistance stays constant as the wick stays fully saturated of working fluid. The lower permeability of the fibre heat pipe will cause regions in the evaporator where no liquid is present (the wick is not fully saturated with working fluid). In these regions, localized vapour blankets will occur, which increase the thermal resistance of the wick.

CONCLUSIONS

An experimental study on three 6 mm OD heat pipes is performed. The working fluid is water, the wick and container material is copper and the length of the heat pipe is 200 mm. The study is basically an assessment of using small diameter fibres (12 μm) as wick material in heat pipes. As the target application is electronics cooling, performance in vertical orientation, both gravity-assisted and gravity-opposing direction, is evaluated. The fibre wick heat pipe is compared to a sintered powder commercially available off-the-shelf heat pipe and a custom made 145 mesh/inch screen heat pipe. Following results are obtained:

- For the gravity-assisted direction, the thermal resistance for heat inputs higher than 60 W the sintered powder heat pipe performs worse, while the screen mesh heat pipe has a lower thermal resistance than the fibre heat pipe. When increasing the heat input, the thermal resistance for the fibre heat pipe increases. This is due to the lower permeability in comparison with the screen mesh. The distribution of the working fluid over the circumference of the wick will be less uniform. Localized vapour blankets will occur when the heat input is increased, increasing the total thermal resistance.
- For the gravity-opposing direction, the thermal resistances for heat inputs higher than 20 W are lower and similar for the screen mesh and the fibre heat pipe. Although generally sintered powder wick can cope with gravity-opposing directions, the screen mesh and fibre heat pipe have larger capillary pressure due to the smaller capillary channels that are created by the dens mesh screen (145 meshes/inch) and smaller fibres (12 μm) that are used. The effect of the higher permeability of the screen mesh is less pronounced compared to the gravity-assisted direction due to the lower heat transfer rate.

REFERENCES

[1] Reay D., McGlen R., Kew P., Heat pipes: theory, design and applications, Butterworth-Heinemann, United Kingdom, 2014.

[2] Kempers R., Ewing D., Ching C.Y., Effect of number of mesh layers and fluid loading on the performance of screen mesh wicked heat pipes, *Applied thermal engineering*, Vol. 26, 2006, pp. 589-595.

[3] Wang Y., Peterson G.P., Investigation of a novel flat heat pipe, *Journal of Heat Transfer*, Vol. 127, 2005, pp. 165-170.

[4] Vasiliev L. L., Review – Heat pipes in modern heat exchangers, *Applied Thermal Engineering*, Vol. 25, 2005, pp. 1-19.

[5] Faghri A., Heat pipes: review, opportunities and challenges, *Frontiers in Heat Pipes 5*, Vol. 1, 2014, pp. 1-48.

[6] Sauciuc I., Mochizuki M., Mashiko K., Saito Y., Nguyen T., The design and testing of the super fiber heat pipes for electronics cooling applications, *Sixtheenth IEEE Semi-ThermTM Symposium*, 2000, pp. 27-32.

[7] ISO, Measurement of fluid flow by means of pressure differential devices – Part 1: orifice plates, nozzles, and venture tubes inserted in circular cross-section conduits running full (ISO 5167-1:1991), Geneva, Switzerland, September 1995.

[8] Moffat R.J., Describing the uncertainties in experimental results, *Experimental Thermal and Fluid Science*, Vol. 1, 1988, pp. 3-17.

[9] Wong S.-C. and Chen C.-W., Visualization experiments for groove-wicked flat plate heat pipes with various working fluids and powder-groove evaporator, *International Journal of Heat and Mass Transfer*, Vol. 66, 2013, pp. 396-403.

[10] Weibel J. A., Garimella S. V., North M. T., Characterization of evaporation and boiling from sintered powder wicks fed by capillary action, *International Journal of Heat and Mass Transfer*, Vol. 53, 2010, pp. 4204-4215.

[11] Li Y., He H. F., Zeng Z. X., Evaporation and condensation heat transfer in a heat pipe with a sintered grooved composite wick, *Applied Thermal Engineering*, Vol. 50, 2013, pp. 342-351.

[12] Weibel J.A. and Garimella S.V., Visualization of vapour formation regimes during capillary-fed boiling in sintered-powder heat pipe wicks, *International Journal of Heat and Mass Transfer*, Vol. 55, 2012, pp. 3498-3510.